J Radioanal Nucl Chem (2014) 299:127–137
DOI 10.1007/s10967-013-2719-0

Measurements of fission yield in 8 MeV bremsstrahlung induced fission of ^{232}Th and ^{238}U

H. Naik · B. S. Shivashankar · H. G. Raj Prakash · Deves Raj · Ganesh Sanjeev · N. Karunakara · H. M. Somashekarappa · S. Ganesan · G. N. Kim · A. Goswami

Received: 1 May 2013 / Published online: 8 October 2013

Abstract The cumulative yields (i.e. the sum of isobaric independent yield up to the isobar of interest) for various fission products have been determined in the 8 MeV bremsstrahlung induced fission of ^{232}Th and ^{238}U by using off-line gamma ray spectrometric technique. From the cumulative yields of the fission products, their mass-chain yields (i.e. the sum of independent yields of all the isobars) were obtained by using charge distribution correction. The mass-chain yields in the ^{232}Th(γ, f) and ^{238}U(γ, f) reactions were compared with the data of similar excitation energy in the ^{232}Th(n, f) and ^{238}U(n, f) reactions to examine the effect of nuclear structure. From these data, it was found that the yields of fission products for the mass numbers 133–134, 138–140 and 143–144 as well as their corresponding complementary products are significantly higher than other fission products. Higher yields of the fission products around the mass numbers 133–134 and 143–144 were explained from the standard I and standard II asymmetric mode of fission, which indicates the role of shell closure proximity. However, the amplitude of yields for the mass numbers 133–134 and 143–144 are reverse in the ^{232}Th(γ, f) and ^{232}Th(n, f) reactions than in the ^{238}U(γ, f) and ^{238}U(n, f) reactions, which has been explained from the point of shell combinations of the complementary fragments.

Keywords Nuclear reactions · ^{232}Th(γ, f) and ^{238}U(γ, f) · $E_\gamma = 8$ MeV bremsstrahlung · Measured fission product yields and mass-chain yield distribution · Off-line γ-spectroscopy using an HPGe detector · Comparison of fission yield between ^{232}Th(γ, f) and ^{238}U(γ, f) reactions

Introduction

Study on mass yield distribution in low energy photon and neutron induced fission of actinides provides information about the effect of nuclear structure and dynamics of descent from the saddle to scission point [1, 2]. This is because

H. Naik (✉) · A. Goswami
Radiochemistry Division, Bhabha Atomic Research Centre, Mumbai 400085, India
e-mail: naikhbarc@yahoo.com

B. S. Shivashankar
Department of Statistics, Manipal University, Manipal 576 104, Karnataka, India

H. G. Raj Prakash
Department of Engineering Physics, JNN College of Engineering, Shimoga 577 204, India

D. Raj · S. Ganesan
Reactor Physics Design Division, Bhabha Atomic Research Centre, Mumbai 400085, India

G. Sanjeev
Department of Studies in Physics, Microtron Centre, Mangalore University, Mangalagangotri, Mangalore 574 199, Karnataka, India

N. Karunakara · H. M. Somashekarappa
University Science Instrumentation Centre, Mangalore University, Mangalagangotri, Mangalore 574 199, Karnataka, India

G. N. Kim
Department of Physics, Kyungpook National University, Daegu 702-701, Republic of Korea

in the photon induced fission, the mass and charge of the compound nucleus is the same, whereas in the neutron induced fission, the compound nucleus mass increase by only one unit. It is a well-known fact that the mass yield distribution [1, 2] in the photon and neutron induced fission of pre-actinides (e.g. Au, Pb, Bi) and heavy-Z actinides (e.g. Es to Lr) are symmetric, whereas for medium-Z actinides (e.g. U to Cf) are asymmetric with double humped. On the other hand, the photon and neutron induced fission of light-Z actinides (e.g. Ac, Th, Pa) are asymmetric with triple humped mass yield distribution [1, 2]. However, with increase of excitation energy and Z of the actinides, the mass yield distribution changes from asymmetric to symmetric and the effect of nuclear structure decreases. Among these, the photon and neutron induced fission of Th–Pa–U and U–Np–Pu are interesting and important for the understanding of basic fission phenomena and from their application in various types of reactors. In particular Th and U are more interesting due to their applications in accelerated driven sub-critical system (ADSs) [3–6], advanced heavy water reactor (AHWR) [7, 8], conventional light and heavy water reactors and fast reactor [9–13]. Besides this, the bremsstrahlung and neutron induced fission of ^{232}Th and ^{238}U at comparable excitation energy near barrier are interesting from the point of view of nuclear structure effect such as role of shell closure proximity and even–odd effect. This is because the bremsstrahlung and neutron induced fission of ^{232}Th and ^{238}U exhibit maximum even–odd effect at excitation energies near fission barrier.

Sufficient data on fission products yields in low energy neutron induced fission of actinides are available in various compilations [14–17]. On the other hand, the fission yield data in the reactor neutron induced fission of ^{232}Th [18–20] and ^{238}U [21, 22] are available in literature. Similarly, fission products yields in mono-energetic neutron [23–47] and photon (bremsstrahlung) [48–73] induced fission of ^{232}Th and ^{238}U are also available in literature. Among these data, the yields of fission products in the bremsstrahlung induced fission of ^{232}Th at 6.5–14 MeV and of ^{238}U at 6.12–11 MeV have been determined by Persyn et al. [55] and Pomme et al. [70], respectively. Their data are based on off-line gamma ray spectrometric technique but only for heavy mass fission products. On the other hand, in the 6.44–13.15 MeV bremsstrahlung-induced fission of ^{232}Th, the yields of fission products are obtained by Piessens et al. [54] by using both physical and off-line gamma ray spectrometric technique. Similarly, in the 6.12–13.15 MeV bremsstrahlung-induced fission of ^{238}U, the yields of fission products are obtained by Pomme et al. [71] by using both physical and off-line gamma ray spectrometric technique. In their data of physical measurement [54, 71], the real picture of mass yield distribution of fission products is not clear due to post-scission neutron emission correction needed for the primary fission fragments. However, from the data based on the off-line gamma ray spectrometric measurement, the effect of nuclear structure is clearly seen. In the neutron- [21, 22, 36–47] and bremsstrahlung- [58–73] induced fission of ^{238}U, it can be seen that the yields of fission products around mass numbers 133–134 are more pronounced compared to mass numbers 143–144. On the other hand, in the neutron [18–20, 23–35] and 6.44–14 MeV bremsstrahlung-[54, 55] induced fission of ^{232}Th, the yields of fission products are more pronounced around mass numbers 143–144 compared to mass numbers 133–134. Thus, there is a different trend of mass yield distribution in the bremsstrahlung induced fission of ^{232}Th and ^{238}U. This can be examined in better way from the mass yield distribution at excitation energy just above the fission barrier. In view of this, in the present work, yields of various fission products in the 8 MeV bremsstrahlung induced fission of ^{232}Th and ^{238}U have been determined by recoil catcher and an off-line γ-ray spectrometric technique by using the Microtron facility at Mangalagangotri University, Mangalore, India. From the yields of the fission products, their mass yield distributions were obtained after charge distribution correction. The present data in the ^{232}Th(γ, f) and ^{238}U(γ, f) reactions are compared with the similar data of comparable excitation energy in the ^{232}Th(n, f) [18–20] and ^{238}U(n, f) [21, 22] reactions to examine the effect of nuclear structure and the one mass unit change of the fissioning system. Besides even–odd effect, the role of standard I and standard II asymmetric mode of fission [74] was also discussed to examine the fine structure of the mass yield distribution. This is because based on the standard I asymmetry mode of fission, the yields of fission products around mass numbers 133–134 and their complementary products are favorable due to the approach of spherical shell at N = 82 [75] in the heavy mass fragments. Similarly, based on standard II asymmetry mode of fission, the yields of fission products around mass numbers 143–144 and their complementary products are favorable due to the approach of deformed shell at N = 88 [75] in the heavy mass fragments.

Experimental details

The experiment was performed by using bremsstrahlung beam with end-point energy of 8 MeV, produced from Microtron accelerator at Mangalore University, India. The bremsstrahlung beam was produced by impinging 8 MeV pulsed electron beam on 0.188 cm thick tantalum target [76]. The Ta target, which acts as an electron to photon converter was located at a distance of 30 cm from the beam exit window.

High-purity Th-metal foil of size 3.36 cm^2 and mass 0.3275 g was wrapped with 0.025 mm thick super pure aluminum foil. Similarly, U-metal foil of thickness 2.7 cm^2 and mass 0.2608 g was wrapped with 0.025 mm thick aluminum foil. They were irradiated separately for 3–4 h with end-point bremsstrahlung energy of 8 MeV. During the irradiation, the Microtron accelerator was operated with pulse repetition rate of 50 Hz and a pulse width of 2.42 µs. The irradiated sample along with aluminum catcher was mounted on a Perspex plate and the gamma rays activities of the fission products were counted by using a 41.1 cm^3 HPGe detector coupled to a PC based 16 K channel analyzer. The resolution of the detector system was 2.0 keV full width at half maximum (FWHM) at the 1332.0 keV γ-line of ^{60}Co. In order to minimize the dead time and coincidence summing effect, appropriate distance between the sample and the detector was chosen for each measurement. The dead time of the detector system during counting was always kept less than 10 %. The γ-ray counting of the sample was done in live time mode and was followed as a function of time. Measurements of the irradiated sample was done for several time with increasing counting time to follow the decay and to have a good counting statistics of the photo-peaks of the gamma rays of different fission products.

Calculation and results

The numbers of detected γ-rays (N_{obs}) of the nuclides of interest were obtained from the photo-peak area, after subtracting the linear Compton background. From the N_{obs} of each individual fission product, their cumulative yields (Y_R) (i.e. the sum of isobaric independent yield up to the isobar of interest) relative to ^{135}I were calculated by using equation [56–58]

$$Y_R = \frac{N_{obs}\left(\frac{CL}{LT}\right)\lambda}{\left[\int_{E_b}^{E_e} n\sigma(E)\Phi(E)dE\right] I_\gamma \varepsilon (1-e^{-\lambda t})e^{-\lambda T}(1-e^{-\lambda CL})} \tag{1}$$

where 'n' is the number of target atoms and σ_F (E) is the photo-fission cross-section of the target nuclei in the bremsstrahlung spectrum with an end-point energy of 8 MeV. Here, $\Phi(E)$ is the photon flux from the fission barrier (E_b) [77] to the end-point energy (E_e). 'ε' and I_γ are the efficiency and branching intensity for the γ-ray of the fission product of interest. 't' and T are the irradiation and cooling times, whereas CL and LT are the clock time and live time of counting, respectively.

During counting, the live time (LT) clock time (CL) differ based on the dead time of the detector system. However, the radioactive nuclide decays based on the clock time. Thus the term (CL/LT) is used for the dead time correction of the observed activity (N_{obs}) and the decay correction term $(1 - e^{-\lambda CL})/\lambda$ is based on the clock time (CL). The term $\int_{E_b}^{E_e} n\sigma_F(E)\Phi(E)dE$ as a whole was obtained using the cumulative yields of ^{135}I (Y_I) from Refs. [55, 70] and using the rearranged Eq. (1) as

$$\int_{E_b}^{E_e} n\sigma(E)\Phi(E)dE = \frac{N_{obs}\left(\frac{CL}{LT}\right)\lambda}{Y_I I_\gamma \varepsilon (1-e^{-\lambda t})e^{-\lambda T}(1-e^{-\lambda CL})}. \tag{2}$$

The nuclear spectroscopic data, such as the γ-ray energy, branching intensity and the half-life of the fission products were taken from Refs. [78, 79]. The cumulative yields (Y_R) of the fission products relative to the fission rate monitor ^{135}I were calculated using Eq. (1). The cumulative yield of ^{135}I in the 8 MeV bremsstrahlung induced fission was taken from Ref. [55]. There is no data available in literature in the 8 MeV bremsstrahlung induced fission of ^{238}U. However, data in the 7.33 and 8.35 MeV bremsstrahlung induced fission of ^{238}U are available in Ref. [70]. Thus we have used the average cumulative value of ^{135}I from the two end-point bremsstrahlung energies of 7.33 and 8.35 MeV. This assumption is reasonable from the point of slight variation of the cumulative yield of ^{135}I in the 6.44–8.35 MeV bremsstrahlung induced fission of ^{238}U [70]. From the cumulative yields (Y_R) of the fission products, their mass chain yields (Y_A) were calculated by using Wahl's prescription of charge distribution [17]. According to this, the fractional cumulative yield (FCY) of a fission product in an isobaric mass chain is given as

$$FCY = \frac{EOF^{a(Z)}}{\sqrt{2\pi\sigma_Z^2}} \int_{-\infty}^{Z+0.5} \exp\left[-\frac{(Z-Z_P)^2}{2\sigma_Z^2}\right] dZ \tag{3}$$

$$Y_A = Y_R/FCY \tag{4}$$

where Z_P is the most probable charge of an isobaric yield distribution. σ_Z is the width parameter and is related to full width at half maximum (FWHM) of the isobaric yield distribution as FWHM $= 2.36\ \sigma_Z$. $EOF^{a(Z)}$ is the even–odd effect with $a(Z) = +1$ for even Z nuclides and -1 for odd Z nuclides.

It can be seen from the above equations that for the calculation of FCY value of a fission product and mass chain yield of an isobaric mass chain, it is necessary to have knowledge of Z_P, σ_Z and $EOF^{a(Z)}$. In the bremsstrahlung-induced fission of ^{232}Th and ^{238}U, the Z_P, σ_Z and $EOF^{a(Z)}$ values can be obtained from the fission yield data of Refs. [55, 70]. On the other hand, there are systematic data on the charge distribution in the reactor neutron-(average $En = 1.9$ MeV) induced fission of ^{232}Th and ^{238}U [80]. The average excitation energies in the 1.9 MeV neutron induced fission of ^{232}Th and ^{238}U are 6.51 and 6.25 MeV, respectively. Similarly, the average excitation energies in the 8 MeV bremsstrahlung induced fission of ^{232}Th and ^{238}U are obtained to be 6.52 and 6.53 MeV, respectively. These values are obtained based on the similar calculation of our earlier work [58]. Thus the excitation energies in the 8 MeV bremsstrahlung- and 1.9 MeV neutron-induced fission of ^{232}Th and ^{238}U are comparable. Further, it can be also seen in Refs. [55, 70, 80] that the average width parameter ($<\sigma_Z>$) in the 8 MeV bremsstrahlung- and reactor neutron-induced fission of ^{232}Th and ^{238}U are nearly the same in spite of the small difference in *N/Z* values of the fissioning systems. In view of this, the average width parameter ($<\sigma_Z>$) values of 0.52 ± 0.08 and 0.55 ± 0.07 from Ref. [80] were used in the 8 MeV bremsstrahlung induced fission of ^{232}Th and ^{238}U, respectively. The mass dependence of the even–odd factor on σ_Z was not considered, which may give rise to an error of 3–5 % in the *FCY* values. The Z_P value of individual mass chain (*A*) for the above fissioning systems was calculated using the relation [17, 81] given below.

$$Z_P = Z_{UCD} \pm \Delta Z_P,\ Z_{UCD} = \frac{Z_F}{A_F}(A + \nu_A) \tag{5}$$

where Z_F and A_F are charge and mass of the fissioning system. Z_{UCD} is the most probable charge based on the unchanged charge density distribution, as suggested by Sugarman and Turkevich [81]. The + and − signs are applicable to light and heavy fragments, respectively. The symbol 'ν_A' is the number of neutrons emitted by the corresponding fragment and is evaluated according to the method of Erten and Aras [82]. Accordingly, ν_A for the light (ν_L) and heavy (ν_H) fission product mass is given as

$$\nu_L = 0.531\nu + 0.062(A_L + 143 - A_F) \tag{6a}$$

$$\nu_H = 0.531\nu + 0.062(A_H - 143). \tag{6b}$$

ΔZ_P is the charge polarization given by Coryell et al. [83] as

$$\nabla Z_P = 0.5(Z_F - 92) + 0.19(A_F - 236) + 0.19(\nu - 2.45) \tag{7}$$

where ν is the average neutron number in the 8 MeV bremsstrahlung-induced fission of ^{232}Th and ^{238}U. The ν values in the 8 MeV bremsstrahlung-induced fission of ^{232}Th and ^{238}U were taken as 2.24 [54] and 2.67 [71], respectively.

The ΔZ_P values obtained in the above way for different mass chains were used in the Eq. (5) to obtain the Z_P value. Then the Z_P and the σ_Z values were used in the Eq. (3) to calculate the FCY values of the individual fission products. Finally, the cumulative yields of the individual fission products and their FCY values were used in Eq. (4) to obtain their mass chain yields data. The cumulative yields of the individual fission products and their mass chain yields in the 8 MeV bremsstrahlung-induced fission of ^{232}Th and ^{238}U along with the nuclear spectroscopic data from Refs. [78, 79] are given in Tables 1 and 2, respectively. The uncertainty shown in the measured cumulative yield of individual fission products in Tables 1 and 2 is the fluctuation of the average value from two determinations with replicate measurements and the counting statistics error. The overall uncertainty represents contributions from both random and systematic errors. The random error in the observed activity is due to counting statistics and is estimated to be 10–15 %, which can be determined by accumulating the data for the optimum period of time, depending on the half-life of the nuclide of interest. On the other hand, the systematic errors are due to the uncertainties in irradiation time (0.2 %), detector efficiency calibration (~3 %), half-life of nuclides of the fission products (~1 %) and the γ-ray abundance (~2 %), which are the largest variation in the literature [78, 79]. Thus, the overall systematic error is about 4 %. An upper limit of error of 11–16 % was determined for the fission product yields based on 10–15 % random error and a 4 % systematic error.

Discussion

The yields of various light mass (A = 77–107) fission products in the 8 MeV bremsstrahlung induced fission of ^{232}Th shown in the Table 1 were determined for the first time, whereas for the heavy mass (A = 127–153) fission products yields are the re-determined values. The yields of heavy mass fission products in the ^{232}Th(γ, f) reaction are in close agreement with the values of Piessens et al. [54] at the end-point bremsstrahlung energy of 8 MeV. However, in their work Piessens et al. [54] have not shown the yields of light mass fission products. In the case of 8 MeV bremsstrahlung induced fission of ^{238}U, the yields of both light mass (A = 84–113) and heavy mass (A = 127–153) fission products shown in Table 2 are determined for the first time. However, the yields of heavy mass (A = 127–153) fission products in the ^{238}U(γ, f) reaction at end-point bremsstrahlung energy of 8 MeV are in close agreement with the average yields from the end-point bremsstrahlung energy of 7.33 and 8.35 MeV [71]. In the work of Pomm'e et al. [71] also the yields of light mass (A = 84–113) fission products were not shown.

It can be seen from Tables 1 and 2 that in the 8 MeV bremsstrahlung induced fission of ^{232}Th and ^{238}U, the yields of fission products around mass numbers 133–134, 138–140 and 143–144 and their complementary products are higher than the other fission products. Similar effect has also been predicted earlier in the bremsstrahlung- [54, 58, 71] and neutron- [18–22] induced fission of ^{232}Th and ^{238}U,

Table 1 Nuclear spectroscopic data and yields of fission products in the 8 MeV photon-induced fission of ^{232}Th ($E^* = 6.52$ MeV)

Nuclide	Half-life	γ-Ray energy (keV)	γ-Ray abundance (%)	Y_R (%)	Y_A (%)
^{77}Ge	11.3 h	264.4	54.0	0.167 ± 0.031	0.169 ± 0.031
^{78}Ge	88.0 min	277.3	96.0	0.351 ± 0.053	0.351 ± 0.053
^{84}Br	31.8 min	881.61	43.0	7.031 ± 0.723	7.045 ± 0.726
		1,616.2	6.2	7.057 ± 0.735	7.071 ± 0.738
^{85}Kr^{m}	4.48 h	151.2	75.0	6.089 ± 0.617	6.113 ± 0.617
		304.9	14.0	6.252 ± 0.629	6.252 ± 0.629
^{87}Kr	76.3 min	402.6	49.6	5.854 ± 0.599	5.913 ± 0.605
^{88}Kr	2.84 h	196.3	25.9	6.414 ± 0.655	6.511 ± 0.664
^{89}Rb	15.2 min	1,032.1	58.0	8.414 ± 0.864	8.414 ± 0.864
		1,248.3	42.6	8.583 ± 0.871	8.583 ± 0.871
^{91}Sr	9.63 h	749.8	23.6	6.180 ± 0.619	6.180 ± 0.619
^{92}Sr	2.71 h	1,024.3	33.0	6.561 ± 0.662	6.561 ± 0.662
		1,384.9	90.0	5.610 ± 0.572	5.661 ± 0.576
^{93}Y	10.18 h	266.9	7.3	4.314 ± 0.457	4.314 ± 0.457
^{94}Y	18.7 min	918.7	56.0	3.686 ± 0.386	3.697 ± 0.386
^{95}Y	10.2 min	954.0	16.0	3.807 ± 0.383	3.842 ± 0.391
^{95}Zr	64.02 days	756.7	54.0	3.862 ± 0.446	3.862 ± 0.446
		724.3	44.2	3.813 ± 0.402	3.813 ± 0.402
^{97}Zr	16.91 h	743.4	93.0	2.754 ± 0.317	2.779 ± 0.319
^{99}Mo	65.94 h	140.5	89.4	1.589 ± 0.171	1.589 ± 0.171
		739.5	12.13	1.767 ± 0.179	1.767 ± 0.179
^{101}Mo	14.61 min	590.1	16.4	1.012 ± 0.188	1.016 ± 0.189
^{103}Ru	39.26 days	497.1	90.0	0.746 ± 0.092	0.746 ± 0.092
^{104}Tc	18.3 min	358.0	89.0	0.574 ± 0.064	0.574 ± 0.064
^{105}Ru	4.44 h	724.4	47.0	0.197 ± 0.026	0.199 ± 0.026
^{105}Rh	35.36 h	319.1	19.2	0.211 ± 0.039	0.211 ± 0.039
^{107}Rh	21.7 min	302.8	66.0	0.058 ± 0.013	0.058 ± 0.013
^{127}Sb	3.85 days	687.0	37.0	0.113 ± 0.021	0.113 ± 0.021
^{128}Sn	59.07 min	482.3	59.0	0.169 ± 0.027	0.172 ± 0.027
^{129}Sb	4.32 h	812.4	43.0	0.440 ± 0.065	0.441 ± 0.065
^{131}Sb	23.03 min	943.4	47.0	1.293 ± 0.204	1.323 ± 0.208
^{131}I	8.02 days	364.5	81.7	1.469 ± 0.231	1.469 ± 0.231
^{132}Te	3.2 days	228.1	88.0	2.634 ± 0.341	2.650 ± 0.344
^{133}I	20.8 h	529.9	87.0	2.980 ± 0.342	2.980 ± 0.342
^{134}Te	41.8 min	566.0	18.0	3.432 ± 0.365	3.639 ± 0.387
		767.2	29.5	3.953 ± 0.441	4.046 ± 0.468
^{134}I	52.5 min	847.0	95.4	4.162 ± 0.451	4.162 ± 0.451
		884.1	65.0	4.420 ± 0.455	4.420 ± 0.455
^{135}I	6.57 h	1,131.5	22.7	4.037 ± 0.406	4.057 ± 0.406
		1,260.4	28.9	4.084 ± 0.443	4.105 ± 0.443
^{137}Xe	3.7 min	455.49	31.0	4.812 ± 0.509	4.812 ± 0.509
^{138}Xe	14.08 min	258.4	31.5	6.196 ± 0.622	6.335 ± 0.637
		434.5	20.3	6.162 ± 0.663	6.301 ± 0.679
^{138}Cs^{g}	33.41 min	1,435.8	76.3	6.816 ± 0.719	6.816 ± 0.719
		1,009.8	29.8	6.727 ± 0.703	6.727 ± 0.703
		462.8	30.7	7.077 ± 0.748	7.077 ± 0.748
^{139}Ba	83.03 min	165.8	23.7	7.536 ± 0.786	7.536 ± 0.786
^{140}Ba	12.75 days	537.3	24.4	7.726 ± 0.837	7.726 ± 0.837
^{141}Ba	18.27 min	190.3	46.0	7.175 ± 0.757	7.197 ± 0.759

Table 1 continued

Nuclide	Half-life	γ-Ray energy (keV)	γ-Ray abundance (%)	Y_R (%)	Y_A (%)
		304.7	35.4	7.088 ± 0.749	7.109 ± 0.751
^{141}Ce	32.5 days	145.4	48.0	7.228 ± 0.761	7.228 ± 0.761
^{142}Ba	10.6 min	255.3	20.5	6.234 ± 0.629	6.278 ± 0.635
^{142}La	91.1 min	641.3	47.0	6.415 ± 0.664	6.415 ± 0.664
^{143}Ce	33.03 h	293.3	42.8	7.743 ± 0.803	7.743 ± 0.803
^{144}Ce	284.89 days	133.5	11.09	7.178 ± 0.738	7.178 ± 0.738
^{146}Ce	13.52 min	316.7	56.0	4.323 ± 0.467	4.336 ± 0.469
		218.2	20.6	4.957 ± 0.539	4.972 ± 0.541
^{146}Pr	24.15 min	453.9	48.0	5.333 ± 0.572	5.333 ± 0.572
		1,524.7	15.6	5.202 ± 0.558	5.202 ± 0.558
^{147}Nd	10.98 days	531.0	13.1	3.285 ± 0.391	3.285 ± 0.391
^{149}Nd	1.728 h	211.3	25.9	1.265 ± 0.142	1.269 ± 0.142
		270.2	10.6	1.277 ± 0.138	1.281 ± 0.138
^{149}Pm	53.08 h	286.0	3.1	1.559 ± 0.137	1.559 ± 0.137
^{151}Pm	53.08 h	340.8	23.0	0.601 ± 0.079	0.601 ± 0.079
^{153}Sm	46.28 h	103.2	30.0	0.180 ± 0.031	0.180 ± 0.031

Y_R cumulative yields, Y_A mass chain yields, ^{135}I fission rate monitor

which support the present observation. The higher yields of the fission products around the mass numbers 133–134 and 143–144 and their complementary products can be explained from the point of view of the standard I and standard II asymmetric fission modes mentioned by Brossa et al. [74], which arise due to shell effects [75]. Based on standard I asymmetry, the fissioning system is characterized by spherical heavy fragment mass with A = 133–134 and $Z_P = 52$ due to the approach of spherical shell closure at N = 82 and a deformed complementary light mass number. Thus the higher yields of the fission products such as ^{133}I and ^{134}Te–^{134}I in the ^{238}U(γ, f) reaction is due to the presence of spherical neutron shell at N = 82. The neutron number of 82 is based on the assumption of one neutron emission for A = 133–134 with most probable charge (Z_P) of 52. Similarly, based on standard II asymmetry, the fissioning system is characterized by a deformed heavy fragment mass with A = 143–144 and $Z_P = 54$ due to the approach of deformed shell closure at N = 88 and slightly deformed light mass. Thus the higher yields of the fission products $^{143-144}$Ce and their complementary products in the ^{232}Th(γ, f) reaction is due to the presence of spherical neutron shell at N = 82. The neutron number of 88 is based on the assumption of 2 neutron emission for A = 143–144 with most probable charge (Z_P) of 56. Thus, the higher yields of fission products ^{133}I and ^{134}Te–^{134}I and their complementary products in the ^{238}U(γ, f) reaction and for ^{143,144}Ce and their complementary products in the ^{232}Th(γ, f) reaction are due to the presence of spherical shell closure at N = 82 and deformed shell closure at N = 88, respectively. Only slight higher yields of the ^{133}I, ^{134}Te–^{134}I and their complementary products in the ^{232}Th(γ, f) reaction and for $^{143-144}$Ce and their complementary products in the ^{238}U(γ, f) reaction will be explained little later. On the other hand, the higher yields of fission products ^{138}Xe–^{138}Cs, $^{139-140}$Ba and their complementary products in both ^{232}Th(γ, f) and ^{238}U(γ, f) reactions are not possible to explain based on only standard I and standard II asymmetric fission modes [74] unless even–odd effect is considered. As can be seen, for the mass numbers 133–134, 138–140 and 143–144, the higher yields of the heavy and light complementary mass fission products are in the interval of five mass and two charge units [80]. As for example, the higher yields of fission products are in the interval of five mass units at A = 133, 138 and 143 or at A = 134, 139 and 144, respectively. The most probable charge corresponding to the masses of 133–134, 138–140 and 143–144 are even Z at 52, 54 and 56, which results the A/Z values of 2.5. Thus the difference of two even charges causes the higher mass chain yields in the interval of five mass units. This indicates the role of even–odd effect besides shell effect.

In order to examine above aspects, the mass chain yields of various fission products in the 8 MeV bremsstrahlung induced fission of ^{232}Th and ^{238}U from present work are plotted in the Fig. 1. Similarly, the mass chain yields data in the reactor neutron induced fission of ^{232}Th [18–20] and ^{238}U [21, 22] from literature are plotted in Fig. 2. This was done because the excitation energy of the 8 MeV bremsstrahlung and reactor neutron induced fission of ^{232}Th and ^{238}U have the comparable excitation energy. The excitation energies for the 8 MeV bremsstrahlung induced fission of ^{232}Th and ^{238}U are 6.52 and 6.53 MeV, respectively. Similarly, the excitation energies for the reactor neutron

Table 2 Nuclear spectroscopic data and yields of fission products in the 8 MeV photon-induced fission of ^{238}U (E* = 6.53 MeV)

Nuclide	Half-life	γ-Ray Energy (keV)	γ-Ray abundance (%)	Y_R (%)	Y_A (%)
^{84}Br	31.8 min	881.61	43.0	0.298 ± 0.051	0.298 ± 0.051
		1,616.2	6.2	0.303 ± 0.061	0.303 ± 0.061
$^{85}Kr^{m}$	4.48 h	151.2	75.0	0.501 ± 0.052	0.503 ± 0.052
		304.9	14.0	0.554 ± 0.093	0.556 ± 0.093
^{87}Kr	76.3 min	402.6	49.6	1.109 ± 0.131	1.115 ± 0.131
^{88}Kr	2.84 h	196.3	25.9	2.765 ± 0.379	2.773 ± 0.381
^{89}Rb	15.2 min	1,032.1	58.0	3.177 ± 0.319	3.177 ± 0.319
		1,248.3	42.6	3.665 ± 0.369	3.665 ± 0.369
^{91}Sr	9.63 h	749.8	23.6	4.582 ± 0.468	4.582 ± 0.468
		1,024.3	33.0	4.911 ± 0.501	4.911 ± 0.501
^{92}Sr	2.71 h	1,384.9	90.0	4.592 ± 0.467	4.615 ± 0.472
^{93}Y	10.18 h	266.9	7.3	3.906 ± 0.396	3.906 ± 0.396
^{94}Y	18.7 min	918.7	56.0	4.246 ± 0.465	4.259 ± 0.466
^{95}Y	10.2 min	954.0	16.0	6.201 ± 0.691	6.232 ± 0.694
^{95}Zr	64.02 days	756.7	54.0	6.795 ± 0.705	6.795 ± 0.705
		724.3	44.2	6.970 ± 0.719	6.970 ± 0.719
^{97}Zr	16.91 h	743.4	93.0	5.998 ± 0.635	6.028 ± 0.637
^{99}Mo	65.94 h	140.5	89.4	4.829 ± 0.524	4.829 ± 0.524
		739.5	12.13	4.679 ± 0.469	4.679 ± 0.469
^{101}Mo	14.61 min	590.1	16.4	7.562 ± 0.773	7.565 ± 0.777
^{103}Ru	39.26 days	497.1	90.0	6.722 ± 0.704	6.722 ± 0.704
^{104}Tc	18.3 min	358.0	89.0	4.058 ± 0.422	4.058 ± 0.422
^{105}Ru	4.44 h	724.4	47.0	2.907 ± 0.381	2.922 ± 0.383
^{105}Rh	35.36 h	319.1	19.2	2.975 ± 0.402	2.975 ± 0.402
^{107}Rh	21.7 min	302.8	66.0	0.697 ± 0.102	0.697 ± 0.102
^{112}Ag	3.13 h	617.5	43.0	0.034 ± 0.008	0.034 ± 0.008
^{113}Ag	5.37 h	298.6	10.0	0.022 ± 0.005	0.022 ± 0.005
^{127}Sb	3.85 days	687.0	37.0	0.152 ± 0.021	0.152 ± 0.021
^{128}Sn	59.07 min	482.3	59.0	0.214 ± 0.033	0.216 ± 0.033
^{129}Sb	4.32 h	812.4	43.0	0.626 ± 0.064	0.627 ± 0.064
^{131}Sb	23.03 min	943.4	47.0	2.402 ± 0.265	2.454 ± 0.271
^{131}I	8.02 days	364.5	81.7	3.181 ± 0.349	3.181 ± 0.349
^{132}Te	3.2 days	228.1	88.0	6.154 ± 0.649	6.185 ± 0.652
^{133}I	20.8 h	529.9	87.0	8.257 ± 0.844	8.257 ± 0.844
^{134}Te	41.8 min	566.0	18.0	7.230 ± 0.732	7.733 ± 0.782
		767.2	29.5	7.182 ± 0.751	7.682 ± 0.803
^{134}I	52.5 min	847.0	95.4	8.655 ± 0.869	8.655 ± 0.869
		884.1	65.0	8.611 ± 0.864	8.611 ± 0.864
^{135}I	6.57 h	1,131.5	22.7	6.921 ± 0.714	6.949 ± 0.714
		1,260.4	28.9	6.175 ± 0.662	6.175 ± 0.662
^{137}Xe	3.7 min	455.49	31.0	5.498 ± 0.553	5.498 ± 0.553
^{138}Xe	14.08 min	258.4	31.5	5.992 ± 0.628	6.114 ± 0.642
		434.5	20.3	5.834 ± 0.627	5.953 ± 0.641
$^{138}Cs^{g}$	33.41 min	1,435.8	76.3	6.399 ± 0.679	6.399 ± 0.679
		1,009.8	29.8	6.558 ± 0.684	6.558 ± 0.684
		462.8	30.7	6.364 ± 0.678	6.364 ± 0.678
^{139}Ba	83.03 min	165.8	23.7	6.926 ± 0.733	6.926 ± 0.733
^{140}Ba	12.75 days	537.3	24.4	6.383 ± 0.663	6.383 ± 0.663

Table 2 continued

Nuclide	Half-life	γ-Ray Energy (keV)	γ-Ray abundance (%)	Y_R (%)	Y_A (%)
^{141}Ba	18.27 min	190.3	46.0	5.435 ± 0.551	5.451 ± 0.554
		304.7	35.4	5.446 ± 0.574	5.462 ± 0.577
^{141}Ce	32.5 days	145.4	48.0	5.562 ± 0.597	5.562 ± 0.597
^{142}Ba	10.6 min	255.3	20.5	4.675 ± 0.503	4.698 ± 0.506
^{142}La	91.1 min	641.3	47.0	4.884 ± 0.523	4.884 ± 0.523
^{143}Ce	33.03 h	293.3	42.8	4.727 ± 0.528	4.727 ± 0.528
^{144}Ce	284.89 days	133.5	11.09	5.105 ± 0.546	5.105 ± 0.546
^{146}Ce	13.52 min	316.7	56.0	2.908 ± 0.293	2.917 ± 0.294
		218.2	20.6	2.845 ± 0.288	2.854 ± 0.289
^{146}Pr	24.15 min	453.9	48.0	3.347 ± 0.363	3.451 ± 0.363
		1,524.7	15.6	3.198 ± 0.362	3.208 ± 0.362
^{147}Nd	10.98 days	531.0	13.1	2.564 ± 0.347	2.564 ± 0.347
^{149}Nd	1.728 h	211.3	25.9	1.621 ± 0.169	1.626 ± 0.169
		270.2	10.6	1.655 ± 0.168	1.659 ± 0.168
^{149}Pm	53.08 h	286.0	3.1	1.734 ± 0.182	1.734 ± 0.182
^{151}Pm	53.08 h	340.8	23.0	0.442 ± 0.059	0.442 ± 0.059
^{153}Sm	46.28 h	103.2	30.0	0.055 ± 0.011	0.055 ± 0.0118

Y_R cumulative yields, Y_A mass chain yields, ^{135}I fission rate monitor

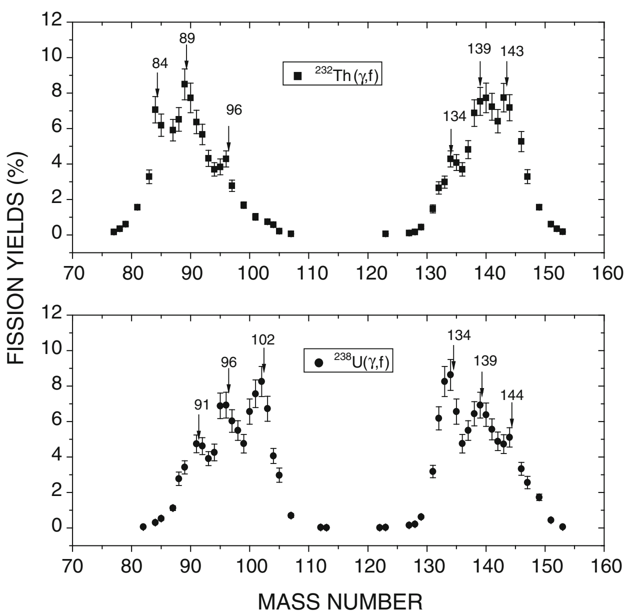

Fig. 1 Plot of post neutron mass chain yields versus mass number in the 8 MeV bremsstrahlung induced fission of ^{232}Th (E* = 6.52 MeV) and ^{238}U (E* = 6.53 MeV)

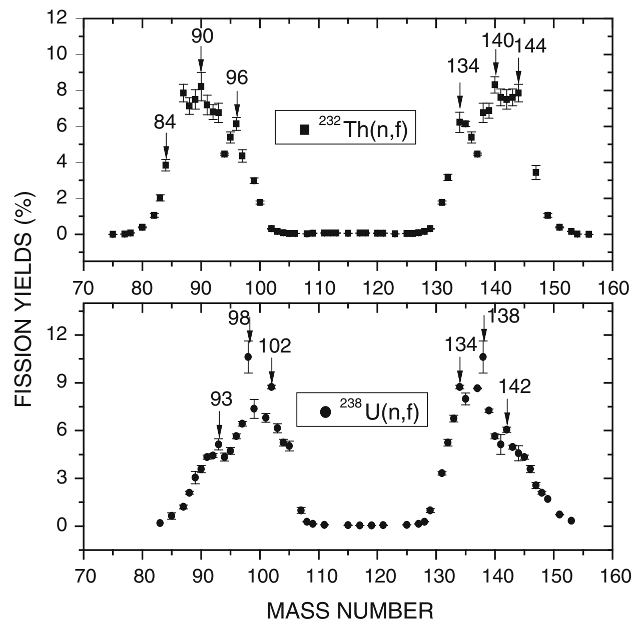

Fig. 2 Plot of post neutron mass chain yields versus mass number in the reactor (average E_n = 1.9 MeV) neutron-induced fission of ^{232}Th [18–20] (E* = 6.51 MeV) and ^{238}U [21, 22] (E* = 6.25 MeV)

induced fission of ^{232}Th and ^{238}U are 6.51 and 6.25 MeV, respectively. This is because the reactor neutron has average neutron energy of 1.9 MeV [21, 22].

It can be seen from Figs. 1 and 2 that the yields of fission products around mass numbers 133–134 and their complementary products are higher in the ^{238}U(γ, f) and ^{238}U(n, f) reactions, whereas they are lower in the ^{232}Th(γ, f) and ^{232}Th(n, f) reactions. Similarly, the yields of fission products around mass numbers 138–140 and their complementary products are higher in the ^{232}Th(n, f) and ^{238}U(n, f) reactions than in the ^{232}Th(γ, f) and ^{238}U(γ, f) reactions. These observations cannot be explainable based on either even–odd effect or standard I and standard II asymmetric mode unless ones consider the effect of complementary shell combinations. Around mass numbers 133–134, the most probable Z is 52 and the fission fragment has spherical 82 n shell if the neutron emission is around one. For the mass numbers 138–140 and 143–144, the most probable Z are 54 and 56, respectively. This corresponds to the deformed 86–88 n shell if the neutron emitted is around one or two. However, the deformed neutron shell are not exactly 88, 64 and 56 but lies between the neutrons number 86–90, 62–66 and 54–58, respectively [75]. In the case of the ^{238}U(γ, f) and ^{238}U(n, f) reactions, for the fragments at A = 134–135 have the complementary fragment at A = 105–103 with probable Z = 40, which correspond to the spherical 82 n and deformed 64 n shell combinations. In the case of the ^{232}Th(γ, f) and ^{232}Th(n, f) reactions, the fragment of A = 134–135 have the complementary A = 99–97 with probable Z = 38, which corresponds to the spherical 82 n shell and 61–59 n without shell. Thus the higher yields of the fission products ^{133}I and ^{134}Te–^{134}I and their complementary products in the ^{238}U(γ, f) and ^{238}U(n, f) reactions are due to spherical 82 n and deformed 64 n shell combination, which is absent in the case of ^{232}Th(γ, f) and ^{232}Th(n, f) reactions. In the ^{238}U(n, f) reaction, for the fragment of A = 139 has the complementary fragment at A = 100 with probable Z = 40, which correspond to the deformed 86 n and 62 n shell combination. Thus in the ^{238}U(n, f) reaction the fission products ^{138}Xe–^{138}Cs and its complementary products have the unusual high yields of about 11 % [21, 22]. Similarly, in the ^{232}Th(n, f) reaction, for the fragment of A = 141 has the complementary fragment at A = 92 with probable Z = 36, which correspond to deformed 87 n and 56 n shell combination. Thus in the ^{232}Th(n, f) reaction, the fission product ^{140}Ba and its complementary product have thehigher yields of 8.2 % [20]. The above facts get support from the observation of very high yields of 10.85 % for ^{144}Ce and ^{84}Br in ^{229}Th (n, f) reaction [84] due to the presence of deformed 88 n and spherical 50 n shell combinations in the complementary pairs. However, in the ^{235}U(n, f) [85] reaction, the yields of ^{143,144}Ce and its complementary product, is not as high as in the case of ^{229}Th (n, f) reaction [84], which is due to the presence of single shell of 86–88 n. These observations clearly indicate the importance of shell combinations in the complementary fragments pairs.

Besides the above facts of shell combination of the complementary fragments, the comparable N/Z of the fragments and fissioning systems also plays its role. As for example, the fragment with A = 139–141 and Z = 54 is favorable from N/Z ratio compared to the fragment at A = 134–135 and 144–145. The fissioning systems ^{232,233}Th* and ^{238,239}U* have the N/Z ratios of 1.578–1.589 and 1.587–1.598, respectively. For the fission products of A = 133–134, 138–140 and 143–144 with most probable Z of 52, 54 and 56 have the N/Z ratios of 1.577, 1.593 and 1.571 in their fragment stage. This is based on the probable neutron to proton ratios of 82/52, 86/54 and 88/56, respectively. The fission products around A = 138–140 and their complementary products have the N/Z ratio of 1.593, which is closer to the value of the fissioning systems ^{232,233}Th* and ^{238,239}U*. Thus the yields of fission products ^{138}Cs and ^{139,140}Ba and their complementary products are higher than adjacent fission products in the fissioning systems ^{232,233}Th* and ^{238,239}U* due the favorable N/Z ratio besides the presence of deformed 86–56 n and 86–62 n shell combinations of the complementary pairs.

Conclusions

1. The yields of various fission products in the 8 MeV bremsstrahlung induced fission of ^{232}Th and ^{238}U have been determined using off-line gamma ray spectrometric technique.
2. In the bremsstrahlung and neutron induced fission of ^{232}Th and ^{238}U, the yields of fission products around A = 133–134, 139–140, 143–144 and their complementary products in the interval of five mass units are higher than other fission products. This indicates the even–odd effect besides the role of shell closure proximity.
3. The higher yields of fission products ^{133}I and ^{134}Te–^{134}I as well as ^{143,144}Ce and their complementary products in the ^{232}Th(γ, f) and ^{238}U(γ, f) reactions are due to the presence of spherical shell at N = 82 and deformed shell at N = 86–88. This is explainable from the point of standard I and standard II asymmetric mode of fission, which indicates the effect of shell closure proximity.
4. The yields of fission products ^{133}I, ^{134}Te–^{134}I and their complementary products are higher in the ^{238}U(γ, f) and ^{238}U(n, f) reactions, whereas they are lower in the ^{232}Th(γ, f) and ^{232}Th(n, f) reactions. This is due to the presence of shell combination in the complementary fragment in the former than later.
5. In the ^{232}Th(γ, f), ^{232}Th(n, f), ^{238}U(γ, f) and ^{238}U(n, f) reactions, the yields of fission products ^{138}Xe–^{138}Cs, ^{139,140}Ba and their complementary products are higher due to the presence of favorable N/Z ratio similar to that of the fissioning systems besides the effect of shell closure proximity.

Acknowledgments The authors express their sincere thanks to the staff of Microtron facility at Mangalgangotri University, Mangalore, India for providing the electron beam to carry out the experiment.

One of the authors (H. Naik) thanks to Dr. V.K. Manchanda, earlier head of Radiochemistry Division for supporting the program and permitting him to visit the Microtron facility to carry out the experiment.

References

1. Vandenbosch R, Huizenga JR (1973) Nuclear fission. Academic, New York
2. Wagemans C (1990) The nuclear fission process. CRC, London
3. Carminati F, Klapisch R, Revol JP, Rubia JA, Rubia C (1993) CERN/AT/93-49 (ET)
4. Rubia C, Rubio JA, Buono S, Carminati F, Fietier N, Galvez J, Geles C, Kadi Y, Klapisch R, Mandrilion P, Revol JP, Roche Ch (1995) CERN/AT/95-44 (ET), (1995) CERN/AT/95-53(ET), (1996) CERN/LHC/96-01 (LET), (1997) CERN/LHC/97-01 (EET)
5. Bowman CD (1994) AIP Conf. Proc. 346, Proceedings of international conference on accelerator-driven transmutation technologies and applications, Las Vegas
6. Accelerator driven systems: energy generation and transmutation of nuclearwaste, status report (Nov 1997) IAEA, Vienna, IAEA-TECDO-985
7. Sinha RK, Kakodkar A (2006) Nucl Eng Des 236:683
8. Ganesan S (2006) Creation of Indian experimental benchmarks for thorium fuel cycle, IAEA coordinated research project on "Evaluated data for thorium–uranium fuel cycle". In: Third research co-ordination meeting, 30 Jan to 2 Feb 2006, Vienna, INDC (NDS)-0494
9. Fast reactors and accelerator driven systems knowledge base, IAEA-TECDOC-1319: thorium fuel utilization: options and Trends
10. Mathieu L et al (2005) "Proportion for a very simple Thorium Molten Salt reactor," In: Proceeding of global international conference, Paper No. 428, Tsukuba
11. Nuttin A, Heuer D, Biliebaud A, Brissot R, Le Brun C, Liatard E, Loiseaux JM, Mathieu L, Meplan O, Merle-Lucotte E, Nifenecker H, Perdu F, David S (2005) Potential of thorium molten salt reactors: detailed calculations and concept evolution with a view to large scale energy production. Proc Nucl Energy 46:77
12. Allen TR, Crawford DC (2007) "Lead-Cooled Fast Reactor Systems and the Fuels and Materials Challenges," science and technology of nuclear installations, Article ID 97486
13. Annual Project Status Report 2000, MIT-ANP-PR-071, INEFL/EXT-2009-00994
14. Rider BF (181) Compilation of fission products yields, NEDO, 12154 3c ENDF-327, Valecicecitos Nuclear Centre
15. England JR, Rider BF (1992) Evaluation and compilation of fission products yields, ENDF/B-VI:1989
16. James M, Mills R, Neutron fission products yields (1993) UKFY2, (1991) JEF-2.2
17. Wahl AC (1988) Atomic Data Nucl. Data Tables 39:1
18. Turkevich A, Nidday JB (1951) Phys Rev 84:52
19. Iyer RH, Mathews CK, Ravindran N, Rengan K, Singh DV, Ramaniah MV, Sharma HD (1963) J Inorg Nucl Chem 25:465
20. Erten HN, Grutter A, Rossler E, von Gunten HR (1981) Nucl Sci Eng 79:167
21. Naik H, Nair AGC, Kalsi PC, Pande AK, Singh RJ, Ramaswami A, Iyer RH (1996) Radiochim Acta 75:69
22. Iyer RH, Naik H, Pandey AK, Kalsi PC, Singh RJ, Ramaswami A, Nair AGC (2000) Nucl Sci Eng 135:227
23. Broom KM (1964) Phys Rev 133:B874
24. Ford GP, Leachman RB (1965) Phys Rev B137:826
25. Ganapathy R, Kuroda PK (1996) J Inorg Nucl Chem 28:2017
26. Tin Mo, Rao MN (1968) J Inorg Nucl Chem 30:345
27. Thein M, Rao MN, Kuroda PK (1968) J Inorg Nucl Chem 30:1145
28. Gevaert LH, Jervis RE, Sharma HD (1970) Can J Chem 48:641
29. Holubarsch W, Pfeiffer L, Gonnenwein F (1971) Nucl Phys A 171:631
30. Swindle DL, Moore DT, Beck JN, Kuroda PK (1971) J Inorg Nucl Chem 33:3643
31. Dubrovina SM, Novgorodlseva VI, Morozov LN, Pchelin VA, Chistjakov LV, Shigin VA, Shubko VM (1973) Report-Yaderno-Fizicheskie Insledovoniya, Report No 16:19
32. Trochon J, Yehia HA, Brisard F, Pranal Y (1979) Nucl Phys A 318:63
33. Glendenin LE, Gindler JE, Ahmad I, Henderson DJ, Meadows JW (1980) Phys Rev C 22:152
34. Lam ST, Yu LL, Fielding HW, Dawson WK, Neilson GC (1983) Phys Rev C 28:1212
35. Simutkin VD, Ryzhov IV, Tutin GA, Vaishnene LA, Blongren J, Pomp S, Oesterlung M, Andersson P, Bevilacqua R, Menlders JP, Prieels R (2010) Conf Proceeding by American Inst Phys USA No. 1175:393
36. Ryzhov IV, Yavshits SG, Tutin GA, Kovalev NV, Saulski AV, Kudryashev NA, Saulski AV, Kudryashev NA, Onegin MS, Vaishnene LA, Gavrikov Yu A, Grudzevich OT, Simutkin VD, Pomp S, Blomgren J, Osterlund M, Andersson P, Bevilacqua R, Meulders J, Prieels R (2011) Phys Rev C 85:054603
37. Borisova NL, Dubrovina SM, Novgorodtseva VI, Pchelin VA, Shigin VA, Shubko VM (1968) Sov J Nucl Phys 6:331
38. Petrzhak VA, Teplykh VF, Panyan MG (1970) Sov J Nucl Phys 11:654
39. Nethaway DR, Mendoza B (1972) Phys Rev C 6:1827
40. Harvey JT, Adams DE, James WD, Beck JN, Meaon JL, Kuroda PK (1975) J Inorg Nucl Chem 37:2243
41. Adams DE, James WD, Beck JN, Kuroda PK (1975) J Inorg Nucl Chem 37:419
42. Rajagopalan M, Pruys HS, Grutter A, Hermes EA, von Gunten HR (1976) J Inorg Nucl Chem 38:351
43. James WD, Adams DE, Beck JN, Kuroda PK (1975) J Inorg Nucl Chem 37:1341
44. Chapman TC, Anzelon GA, Spitale GC, Nethaway DR (1978) Phys Rev C 17:1089
45. Nagy S, Flynn KF, Gindler JE, Meadows JW, Glendenin LE (1978) Phys Rev C 17:163
46. Afarideh A, Annole KR (1989) Ann Nucl Energy 16:313
47. Lhersonnau G, Denloov P, Canchel G, Huikari J, Jardin J, Tokinen A, KOlhinen V, Lau C, Lebroton L, Mueller AC, Nieminen A, Nummela S, Penttila H, Perajavi K, Radivojevic Z, Rubchenya V, Saint-Laurent MG, Trzaska WH, Vakhtin D, Vervier J, Villari AC, Viang JC, Aystoe J (2000) Eur Phys J A (Hadron and Nuclei) 9:385
48. Hiller DM, Martin DS Jr (1953) Phys Rev 90:581
49. Gevaert LH, Jervis RE, Subbarao SC, Sharma HD (1970) Can J Chem 48:652
50. Schrøder B, Nydahl G, Forkman B (1970) Nucl Phys A 143:449
51. Chattopadhyay A, Dost KA, Krajbich I, Sharma HD (1973) J Inorg Nucl Chem 35:2621
52. Hogan JC, Richardson AE, Meason JL, Wright HL (1977) Phys Rev C 16:2296
53. Gunther W, Huber K, Kneissl U, Krieger H, Maier HJ (1980) Z Phys A 295:333
54. Piessens M, Jacobs E, Pomm′e S, De Frenne D (1993) Nucl Phys A 556:88
55. Persyn K, Jacobs E, Pomme S, De Frenne D, Govaert K, Yoneama M-L (1997) Nucl Phys A 620:171
56. Naik H, Nathaniel TN, Goswami A, Kim GN, Lee MW, Suryanarayana SV, Ganesan S, Kim EA, Cho M-H, Ramakumar KL (2012) Phys Rev C 85:024623

57. Naik H, Goswami A, Kim GN, Lee MW, Kim KS, Suryanarayana SV, Kim EA, Shin SG, Cho M-H (2012) Phys Rev C 86:054607
58. Naik H, Nimje VT, Raj D, Suryanarayana SV, Goswami A, Singh S, Acharya SN, Mttal KC, Ganesan S, Chandrachoodan P, Manchanda VK, Venugopal V, Banarjee S (2011) Nucl Phys A 853:1
59. Schmitt RA, Sugarman N (1954) Phys Rev 95:1260
60. Richter HG, Coryell CD (1954) Phys Rev 95:1550
61. Katz L, Kavanagh TM, Cameron AGW, Bailey EC, Spinks JWT (1958) Phys Rev 99:98
62. Meason JL, Kuroda PK (1966) Phys Rev 142:691
63. Willams IR, Fulmer CB, Dell GF, Engebretson MJ (1968) Phys Lett B 26:140
64. Swindle D, Wright R, Takahashi K, Rivera WH, Meason JL (1973) Nucl Sci Eng 52:466
65. James WD, Adams DE, Sigg RA, Harvey JT, Meason JL, Beck JN, Kuroda PK, Wright HL, Hogan JC (1978) J Inorg Nucl Chem 38:1109
66. Thierens H, De Frenne D, Jacobs E, De Clercq A, D'hondt P, Deruytter AJ (1976) Phys Rev C 14:1058
67. Jacobs E, Thierens H, De Frenne D, De Clercq A, D'hondt P, De Gelder P, Deruytter AJ (1979) Phys Rev C 19:422
68. De Clercq A, Jacobs E, De Frenne D, Thierens H, D'hondt P, Deruytter AJ (1976) Phys Rev C 13:1536
69. Jacobs E, De Clercq A, Thierens H, De Frenne D, D'hondt P, De Gelder P, Deruytter AJ (1979) Phys. Rev C 20:2249
70. Pomme S, Jacobs E, Persyn K, De Frenne D, Govaert K, Yoneama ML (1993) Nucl Phys A 560:689
71. Pomm'e S, Jacobs E, Piessens M, De Frenne D, Persyn K, Govaert K, Yoneama M-L (1994) Nucl Phys A 572:237
72. Yamadera A, Kase T, Nakamura T (1988) In: Proceedings of the international conference on nuclear data for science and technology, Moto (Japan Atomic Energy Research Institute, Tokai, 1988) p 1147
73. Gook A, Chernykh M, Eekardt C, Enders J, von Neumann-Cosel P, Oberstedt A, Oberestedt S, Richter A (2011) Nucl Phys A 851:1
74. Brossa U, Grossmann S, Muller A (1990) Phys Rep 197:167
75. Wilkins BD, Steinberg EP, Chasman RR (1976) Phys Rev C 14:1832
76. Eshwarappaa KM, Ganesh S, Yogesh K, Sinha A, Sarkar PS, Godwal BK (2005) Nucl Inst Methods Phys Res A 540:412
77. Bjornholm S, Lynn JE JE (1980) Rev Mod Phys 52:725
78. Browne E, Firestone RB, Shirley VS (ed) (1986) Table of radioactive isotopes; In: Firestone RB, Ekstrom LP: WWW Table of radioactive isotopes Ver 2.1, available at http://ie.lbl.gov.toi/
79. Blachot J, Fiche Ch (1981) Table of radioactive isotopes and their main decay characteristics. Ann Phys (Paris) 6:3–218
80. Naik H, Singh RJ, Iyer RH (2003) Eur Phys J A 16:495
81. Sugarman N, Turkevich A, Coryell CD, Sugarman N (eds.) (1951) In: Radiochemical studies: the fission product, McGraw-Hill, New York, p 1396
82. Erten HN, Aras NK (1979) J Inorg Nucl Chem 41:149
83. Coryell CD, Kaplon M, Fink RD (1961) Can J Chem 39:646
84. Agarwal C, Goswami A, Kalsi PC, Singh S, Mhatre A, Ramaswami A (2008) J Radioanal Nucl Chem 275:445
85. Metz LA, Frise JJ, Finn EC, Greenwood LR, Kephart RF, Hines CC, King MD, Henry KM, Wall DE (2013) J Radioanal Nucl Chem 296:763